# Differential Interferometric Synthetic Aperture Radar-Based Landslide Monitoring: A Case Study of Wayanad, India

Manvi Kanwar[1][a] and Samsung Lim[2][b]
[1]School of Civil and Environmental Engineering, University of New South Wales, Australia
[2]Associate Professor, School of Civil and Environmental Engineering, University of New South Wales, 2052, Australia

Keywords: Rainfall-Induced Landslides, D-Insar, Sentinel-1, Remote Sensing.

Abstract: On July 30th, 2024, the Wayanad region of Kerala, India, experienced a devastating landslide triggered by intense monsoon rainfall. This event highlighted the region's need for effective landslide monitoring and early warning systems. Differential Interferometric Synthetic Aperture Radar (DInSAR) is a powerful and efficient remote sensing technique for detecting ground deformation and monitoring landslides. This study utilizes Sentinel-1 SAR images to monitor the Wayanad landslide by processing and analyzing SAR data using the DInSAR technique to identify ground displacement patterns. The results demonstrate the effectiveness of DInSAR in capturing pre- and post-event deformations, offering valuable insights into the landslide dynamics. This study underscores the potential of SAR-based real-time landslide monitoring and risk mitigation in landslide-prone regions.

## 1 INTRODUCTION

Wayanad, a district in Kerala's Western Ghats, India, is highly susceptible to landslides, a hazard exacerbated by both natural and anthropogenic factors. The region's topography, characterized by elevated slopes and a soil cover consisting mainly of boulders, colluvium, and laterite, combined with the region's propensity for heavy monsoon rainfall, makes it particularly vulnerable to landslide events (Kuriakose et al., 2009). On July 30th, 2024, a massive rainfall event which brought over 14 cm of rain in a single day — 493% above the average — triggered multiple landslides in Chooralmala, Mundakkai, and Vellarimala villages (Mishra, 2024). These landslides are not isolated; Wayanad has a history of similar events, such as the over 3,000 landslides reported during the 2018 floods and the multiple landslides in Puthumala in 2019 (National Remote Sensing Centre, 2023).

While natural factors such as topography and rainfall primarily contribute to landslides, anthropogenic activities have increasingly significantly exacerbated these events. Studies following the 2018 and 2019 floods identified extensive land-use changes, particularly the establishment of tea and rubber plantations and the construction of houses and other infrastructure in landslide-prone areas (Premlet B, 2019). These activities obstruct natural drainage systems and saturate the soil, making it more susceptible to landslides during heavy rains. Moreover, the velocity of rivers such as Iruvazhinji, which runs through steep terrain before descending rapidly in elevation, can intensify the impact of floods and landslides.

Kerala's Western Ghats, including Wayanad, have long been recognised as vulnerable. In 2011, the Madhav Gadgil-led Western Ghats Ecology Expert Panel recommended that a sizeable portion of the Western Ghats, including areas in Wayanad, be designated as Ecologically Sensitive Zones (ESZ) (Gadgil Madhav, 2011). This designation would have restricted industrial activities, mining, and construction in these areas. However, these recommendations were not implemented, exposing the region to the ongoing risks of landslides and other environmental disasters.

In areas affected by excessive rainfall, using optical images to determine landslide extent can be severely hindered by cloud cover and adverse weather conditions. However, microwave-based Synthetic

[a] https://orcid.org/0009-0006-6680-6068
[b] https://orcid.org/0000-0001-9838-8960



Kanwar, M. and Lim, S.
Differential Interferometric Synthetic Aperture Radar-Based Landslide Monitoring: A Case Study of Wayanad, India.
DOI: 10.5220/0013080700003935

In *Proceedings of the 11th International Conference on Geographical Information Systems Theory, Applications and Management (GISTAM 2025)*, pages 113-120
ISBN: 978-989-758-741-2; ISSN: 2184-500X

Aperture Radar (SAR) images offer a significant advantage in such scenarios. Unlike optical imagery, SAR can penetrate clouds and provide consistent data irrespective of weather conditions, making it an invaluable tool for monitoring large and inaccessible areas quickly and reliably. This advantage is evident in recent studies (Debevec Jordanova et al., 2024; Lau et al., 2024), demonstrating DInSAR's utility in mapping and monitoring landslides. Similarly, this research applies DInSAR to assess the Wayanad landslide, a rainfall-induced event, by leveraging the phase differences between SAR images captured at different times. While other studies have used advanced techniques like SBAS or integrated in-situ monitoring, this study focuses on rapid assessment of ground deformation using Sentinel-1 SAR data, which is freely accessible. This approach offers valuable insights into hazard assessment and disaster management, allowing response teams to prioritise the most vulnerable areas and overcome the limitations of traditional optical methods.

## 2 STUDY AREA

Wayanad District, located in the northeastern part of Kerala, India, is known for its diverse geography and significant natural beauty. The district is characterized by its hilly terrain, with elevations ranging from 700 to 2,100 meters above sea level and is part of the Western Ghats Mountain range. Wayanad's landscape includes dense forests, lush green tea and coffee plantations, and numerous rivers and waterfalls. The region experiences a tropical monsoon climate, with an average annual rainfall of 2,500 to 3,000 millimetres (India Meteorological Department, 2024), contributing to its rich biodiversity and dense vegetation. It is bordered by the districts of Kannur to the west, Kozhikode to the south, and Malappuram to the southwest. To the east, Wayanad shares its boundaries with the state of Karnataka. The district's geographical and climatic conditions make it highly susceptible to landslides, particularly during the monsoon season, which highlights the importance of effective monitoring and disaster management in the region. The present study focuses on one sub-swath of a Sentinel-1 SAR image, which encapsulates approximately 20,825 km² of area, as shown in Figure 1.

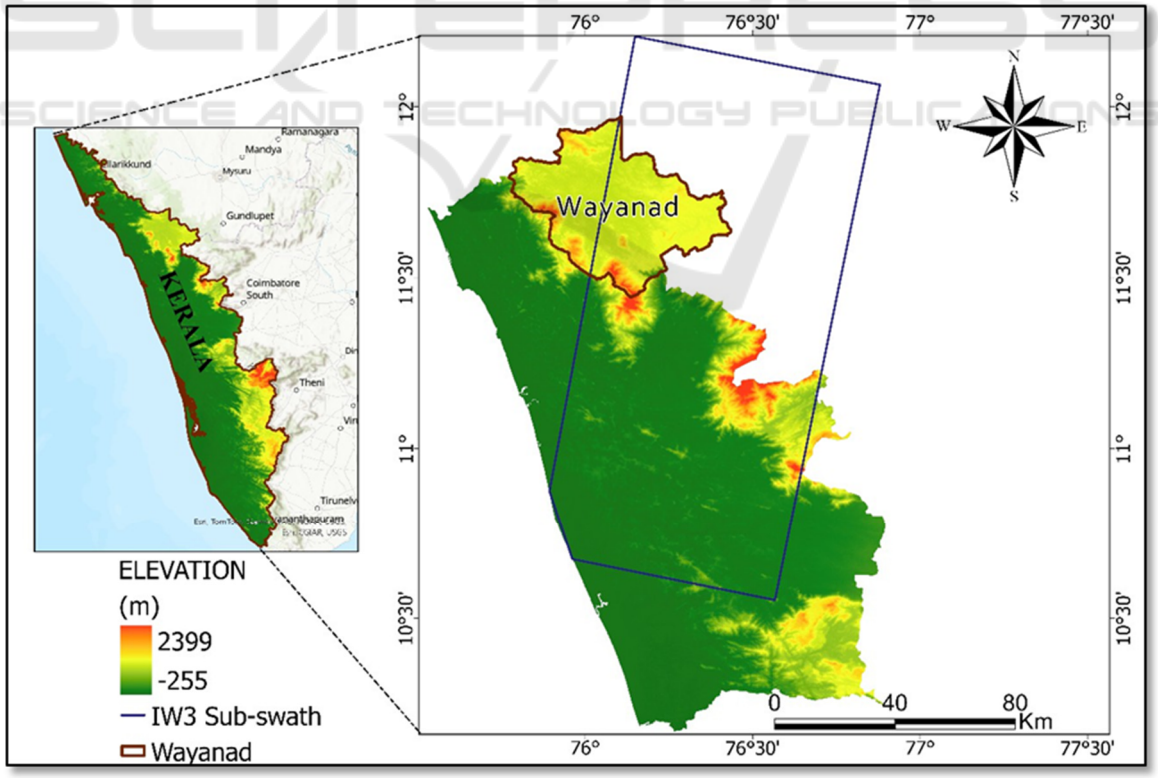


Figure 1: Study Area.

Table 1: Data Characteristics of the Pre-Event Sar Images Using Stack Overview in Snap.

| Acquisition date | Track | Orbit | Temporal Baseline (days) | Perpendicular Baseline (m) | Modelled Coherence |
|---|---|---|---|---|---|
| 8 July 2024 (reference) | 165 | 54662 | 0 | 0 | 1 |
| 20 July 2024 (secondary) | 165 | 54837 | 12 | -123 | 0.89 |

Table 2: Data Characteristics of the Post-Event Sar Images Using Stack Overview in Snap.

| Acquisition date | Track | Orbit | Temporal Baseline (days) | Perpendicular Baseline (m) | Modelled Coherence |
|---|---|---|---|---|---|
| 1 August 2024 (reference) | 165 | 55012 | 0 | 0 | 1 |
| 13 August 2024 (secondary) | 165 | 55187 | 12 | -142 | 0.87 |

# 3 METHODOLOGY

## 3.1 Data Acquisition

This research leverages SAR datasets obtained from the Sentinel-1A and 1B missions, launched in 2014 and 2016. These satellites are equipped with C-band SAR technology, which offers open-access data capable of capturing Earth's surface imagery under all weather conditions, day and night. Sentinel-1 provides data well suited for medium-resolution applications, with a revisit period of 12 days, allowing for extensive area coverage. The satellites operate in the Interferometric Wide (IW) swath mode, utilizing Terrain Observation by Progressive Scans (TOPS) to achieve a ground coverage of approximately 250 km. The geometric resolution of the SAR products is 5 m by 20 m in range and azimuth, respectively.

For the application of the D-InSAR method, two images were acquired before the landslide event happened, and two were after the Wayanad landslide to demonstrate the changes in the landform. Data processing was performed using SeNtinel Applications Platform (SNAP) version 10.0.0, a free software provided by the European Space Agency (ESA). The SAR data was sourced from the Alaska Satellite Facility (ASF) and provided by the European Space Agency (2023) as part of the Sentinel-1 mission. Each Sentinel-1 Single Look Complex (SLC) product consists of three Interferometric Wide Swaths (IW1, IW2, and IW3) and nine bursts. The IW3 sub-swath was selected for this study as it encompasses the area of interest. The acquired images were in both VH and VV polarization modes. Tables 1 and 2 present the features of the pre-event and post-event datasets, respectively.

The perpendicular baseline was kept within 200 meters to maintain data quality. This restriction helps ensure accurate interferometric measurements and reliable results in SAR data processing. The perpendicular baseline is a critical parameter in SAR interferometry, affecting the interferograms' spatial resolution and coherence (Li & Bethel, 2008). Keeping it within this limit helps minimize errors and maintain the overall quality of the interferometric data (Zhang et al., 2005).

## 3.2 Preprocessing

Preprocessing of the Sentinel-1 SAR data involves several steps to ensure the accuracy of the DInSAR analysis:

**Orbit File Application:** Accurate orbit data are applied to the SAR images to correct for satellite position errors. Precise orbit files provided by ESA were utilized to ensure accurate geolocation and alignment of the Sentinel-1 imagery.

**Radiometric Calibration**: This step involves converting the SAR image data from digital numbers (DN) to radar backscatter intensity, which is essential for quantitative analysis.

**Multilooking:** The SAR images are multilooked to reduce speckle noise inherent in SAR data by averaging adjacent pixels. This study used a multi-look factor of 4 in range and 1 in azimuth, reducing noise while maintaining spatial resolution suitable for analyzing landslide deformation.

**Co-registration:** Pre and post-event SAR images are precisely aligned to ensure accurate phase difference calculations. This step minimizes phase errors due to misalignment.

**Interferogram Generation:** An interferogram is generated by computing the phase difference between the co-registered SAR images. This interferogram represents the ground displacement in the radar line of sight (LOS).

### 3.3 DInSAR Processing

The core of the DInSAR technique involves the following steps:

**Phase Unwrapping:** The interferometric phase is wrapped between -π and π, necessitating a phase unwrapping process to retrieve the actual displacement values. The Statistical-cost Network-flow Algorithm for Phase Unwrapping (SNAPHU) algorithm is commonly used. This study employed SNAPHU with a coherence mask to restrict unwrapping to areas with a coherence threshold of 0.3, ensuring accurate displacement retrieval in high-coherence regions.

**Topographic Phase Removal:** The influence of topography on the interferometric phase is removed using a Digital Elevation Model (DEM), such as the Shuttle Radar Topography Mission (SRTM) DEM, to isolate the phase related to ground deformation. A 30 m resolution SRTM DEM was used in this study to ensure the precise removal of the topographic component in the Wayanad region, characterized by hilly terrain.

**Temporal and Spatial Filtering:** Temporal and spatial filtering techniques reduce noise and enhance the signal related to ground deformation. With an adaptive window size of 32 x 32 pixels, the Goldstein filter preserves deformation-related signals while reducing noise.

**Displacement Map Generation:** The unwrapped phase is converted into displacement maps representing the ground movement in the radar LOS direction. These maps are then geocoded to produce spatially accurate deformation maps. This study projected the displacement maps onto the WGS84 coordinate system for spatial analysis and visual interpretation of ground deformation pattern.

## 4 RESULTS AND DISCUSSIONS

The results obtained after the dataset's preprocessing demonstrate the landform change before and after the event. The LOS displacement and coherence maps were generated. This analysis helps us showcase the land movement that happened towards or away from the radar line of sight. P et al. (2025) used machine learning models to determine the landslide susceptibility in the Wayanad district and found that the western part was most susceptible to landslides. Thus, the coherence and displacement values of these areas are discussed.

The observation from the Maps in Figures 2 to 5 from the estimated coherence suggests several important conclusions:

### 4.1 Coherence Analysis

**Before the Landslide:** The pre-landslide surface stability of the Wayanad region is evident from the coherence map in Figure 2, where 57.8% of the pixels exhibit coherence values above 0.6. This indicates predominantly stable ground. 25.3% of the region displays high coherence values (0.8–1.0), typically associated with undisturbed surfaces like rocky terrain or dense vegetation. Such areas reflect minimal displacement or deformation.

Conversely, regions with coherence values below 0.4, constituting 15.7% of the pixels, primarily occur in riverbeds and forested areas, as seen from the histogram in Figure 3. These zones experience temporal decorrelation due to vegetation growth, soil moisture variations, or minor ground movements, which are unstable precursors. Some areas' relatively lower coherence values (0–0.53) suggest potential surface instability or subtle deformations, even before the landslide event.

**After the Landslide:** Following the landslide triggered by intense monsoon rainfall, significant displacement and surface disruption are observed, particularly in areas near **Mundakkai Hills**, **Punchrimattom**, **Mundakkai**, and **Chooralmala** (Figure 4). These locations were selected for monitoring due to their proximity to steep slopes, historical landslide occurrences, and the presence of vulnerable settlements and infrastructure.

The coherence values in these regions decreased notably, reflecting ground instability and displacement. At **Mundakkai Hills**, coherence dropped from an average of 0.75 (pre-event) to 0.42 (post-event). Similarly, **Punchrimattom** experienced

a reduction from 0.81 to 0.46, and **Mundakkai** decreased from 0.84 to 0.48. The most severe displacement occurred near **Chooralmala**, where coherence dropped from 0.77 to 0.32, indicating significant material flow and surface disruption.

Figure 5 demonstrates only 34.2% of the pixels-maintained coherence above 0.6 after the landslide, compared to 57.8% before the event. Regions with coherence values in the range of 0.2–0.4 increased significantly, from 9.8% (pre-event) to 28.6% (post-event), indicating widespread ground displacement. Additionally, areas with coherence below 0.2, representing 12.3% of the pixels, correspond to zones of extreme surface disturbance caused by material displacement during the landslide.

The spatial analysis of displacement highlights the utility of SAR-based techniques in mapping and quantifying ground movement. The coherence maps provide a reliable measure of surface stability, with changes in coherence values reflecting the severity and extent of the landslide. These findings align with observations by (Ferretti et al., 2001), who emphasized the effectiveness of SAR coherence analysis in monitoring ground deformation following natural disasters.

From all above, it can be observed that the coherence analysis underscores the substantial alterations in surface properties caused by the landslide, with significant changes in coherence values reflecting both the extent of the ground displacement and the areas of severe surface disturbance. These results are critical for understanding the landslide's overall impact, as they provide detailed insights into the spatial distribution of ground instability and the transformation of surface conditions. The observed increase in coherence in certain regions post-event suggests the exposure of more stable and homogeneous surfaces, likely due to the compaction and redistribution of material during the landslide. This analysis highlights the event's severity and establishes a reliable foundation for developing future monitoring strategies, enabling better risk assessment, mitigation efforts, and informed planning for disaster-prone regions.

## 4.2 Displacement and Surface Stability

Figures 6 and 7 illustrate the LOS displacement maps of the Wayanad region before and after the landslide event, respectively. These maps provide critical insights into the extent and movement of the landslide as detected by the radar system. The LOS displacement, measured in the radar line-of-sight direction, highlights surface movement both towards and away from the radar sensor.

***Before the Landslide*:** The displacement map before the event, shown in Figure 6, indicates stable surface conditions with relatively uniform displacement values across the region. Displacement values predominantly range between -0.0014 m and 0.0048 m, suggesting minor ongoing ground movement potentially related to environmental or geological activity. Areas such as Mundakkai Hills, Punchrimattom, and Chooralmala exhibit minimal displacement, underscoring the absence of significant pre-event deformation.

***After the Landslide*:** The post-event displacement map, shown in Figure 7, demonstrates substantial changes in surface movement triggered by the landslide. Negative displacement values (presented in blue) represent movement away from the radar sensor and are prominently observed in the areas most impacted by the landslide, such as Chooralmala. Maximum negative displacement values reach approximately -0.0118 m, reflecting the material's downward and outward movement from the hillside during the landslide's initiation. In contrast, high positive displacement values (depicted in yellow) correspond to regions where the surface moved towards the radar sensor, likely indicating debris accumulation. This phenomenon is evident in the towns of Mundakkai and Chooralmala, where positive displacement values of up to 0.0118 m are observed, suggesting debris flow and subsequent compaction. The displacement maps effectively capture the dynamic nature of the landslide. The pre-event SAR images reveal small-scale displacements indicative of ongoing ground activity, while the post-event deformation map highlights pronounced changes resulting from the landslide. The stark contrast between the negative and positive displacement values represents the landslide's impact, illustrating the initiation of material flow from the hillside and the accumulation of debris in surrounding areas, including Mundakkai and Chooralmala. These results underscore the utility of InSAR-derived LOS displacement data in detecting and quantifying surface changes. The analysis demonstrates the radar system's capability to track the landslide's initiation and the subsequent debris flow, providing valuable insights into the event's impact and progression.

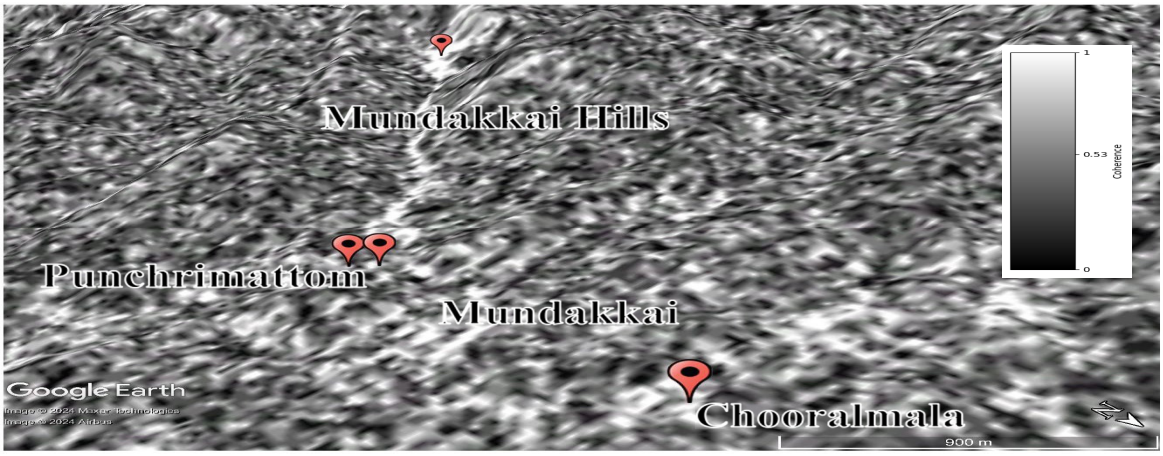


Figure 2: Coherence monitored before the landslide event.

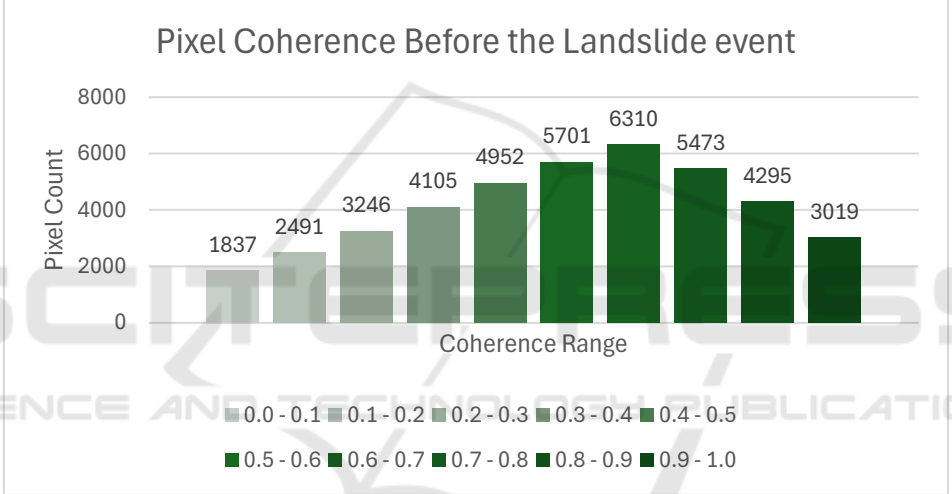


Figure 3: Pixel-based analysis of coherence before the landslide event.


Figure 4: Coherence monitored after the landslide event.

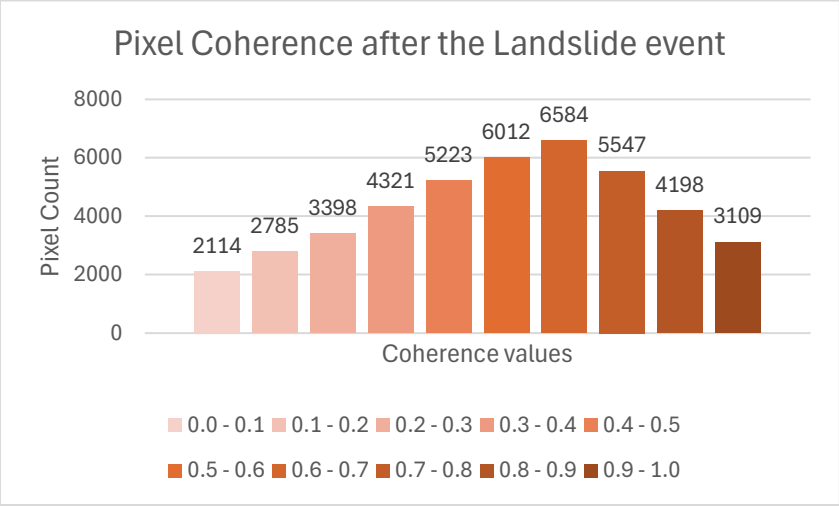


Figure 5: Pixel-based analysis of coherence after the landslide event.

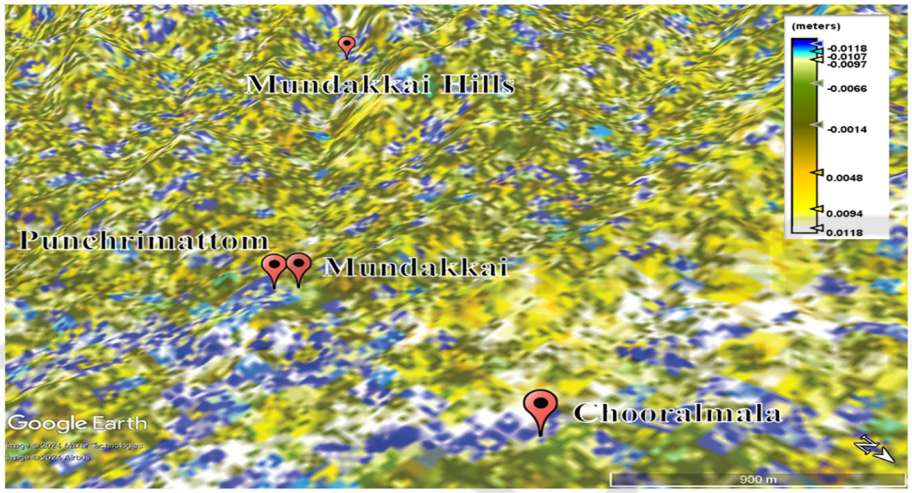


Figure 6: Displacement towards radar LOS before the landslide event.

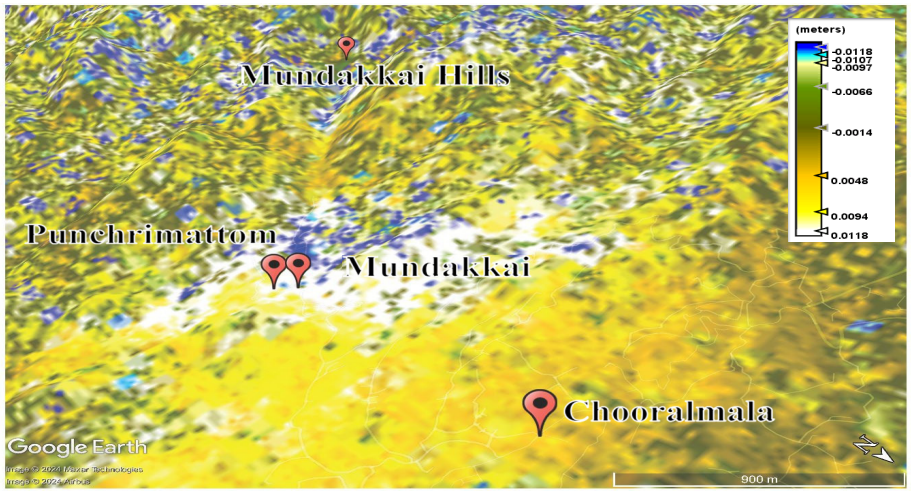


Figure 7: Displacement towards radar LOS after the landslide event.

# 5 CONCLUSION

This study demonstrated the successful application of DInSAR using Sentinel-1 SAR data to monitor the Wayanad landslide of July 30, 2024. By analyzing four SAR images captured before and after the event, coherence and LOS displacement maps were generated, providing a detailed assessment of the landslide's extent and dynamics. The pre-event coherence map revealed stable surface conditions, with 57.8% of pixels maintaining coherence above 0.6. In contrast, the post-event coherence map indicated significant ground deformation, with coherence values above 0.6 dropping to 34.2% and regions with coherence below 0.2 increasing to 12.3%. These changes highlight the substantial disturbance caused by the landslide.

The LOS displacement map further quantified surface movement, with negative values (up to -0.011 m) reflecting downward displacement in the affected areas and positive values indicating debris accumulation. This displacement pattern revealed the spatial dynamics of the landslide, from initial material displacement to subsequent debris deposition in the Mundakkai, Punchrimattom, and Chooralmala regions.

Triggered by slope instability due to intensified rainfall, the Wayanad landslide demonstrates the utility of DInSAR for rapid and accurate assessment of rainfall-induced landslides. The technique effectively detected and quantified ground deformation, providing critical insights into the event's mechanisms and extent. These results emphasize the importance of integrating SAR-based remote sensing into landslide monitoring systems, enabling timely assessments for emergency response and long-term hazard mitigation. Future studies could incorporate advanced InSAR techniques to monitor the annual rate of slope movement and improve early warning systems in regions prone to recurring landslides. This research highlights the potential of DInSAR to enhance our understanding of landslide dynamics and support disaster management efforts in vulnerable areas.

# REFERENCES


Debevec Jordanova, G., Popović, Z., Yastika, P. E., Shimizu, N., Oštir, K., & Verbovšek, T. (2024). SBAS DInSAR and in situ monitoring of the Šumljak landslide (SW Slovenia) dynamics driven by rainfall and piezometric-level fluctuation. *Landslides*. https://doi.org/10.1007/s10346-024-02408-4

European Space Agency (ESA). SNAP-Sentinel Application Platform, v.10.0.0. https://step.esa.int/main/toolboxes/snap.

Ferretti, A., Prati, C., & Rocca, F. (2001). Permanent scatterers in SAR interferometry. *IEEE Transactions on Geoscience and Remote Sensing*, *39*(1), 8–20. https://doi.org/10.1109/36.898661

Gadgil Madhav. (2011). *Report of the Western Ghats Ecology Expert Panel Part I*.

India Meteorological Department. (2024). *Cumulative Rainfall For Kerala-Sw Monsoon 2024*.

Kuriakose, S. L., Sankar, G., & Muraleedharan, C. (2009). History of landslide susceptibility and a chorology of landslide-prone areas in the Western Ghats of Kerala, India. *Environmental Geology*, *57*(7), 1553–1568. https://doi.org/10.1007/s00254-008-1431-9

Lau, R., Seguí, C., Waterman, T., Chaney, N., & Veveakis, M. (2024). InSAR-informed in situ monitoring for deep-seated landslides: insights from El Forn (Andorra). *Natural Hazards and Earth System Sciences*, *24*(10), 3651–3661. https://doi.org/10.5194/nhess-24-3651-2024

Li, Z., & Bethel, J. (2008). *Image Coregistration In Sar Interferometry*.

Mishra, A. (2024, August 1). *Explained with maps: How topography, human density led to devastation in Kerala's Wayanad*. The Print. https://theprint.in/theprint-essential/explained-with-maps-how-topography-human-density-led-to-devastation-in-keralas-wayanad/2202631/

National Remote Sensing Centre, I. S. R. O. (2023). *Landslide Atlas of India (Mapping, Monitoring and R&D studies using Remote Sensing data)*. https://www.nrsc.gov.in

P, L., C, M., Mathew, A., & Shekar, P. R. (2025). Machine learning and deep learning-based landslide susceptibility mapping using geospatial techniques in Wayanad, Kerala state, India. *HydroResearch*, *8*, 113–126. https://doi.org/10.1016/j.hydres.2024.10.001

Premlet B. (2019). *Landslides In Kerala 2018 Chair, Educational activities IEEE Kerala Section* (Vol. 23).

Zhang, H., Zeng, Q., Liu, Y., Li, X., & Gao, L. (2005). *The Optimum Selection of Common Master Image for Series of Differential SAR Processing to Estimate Long and Slow Ground Deformation*. *Master Image for Series of Differential SAR Processing to Estimate Long and Slow Ground Deformation*. http://dx.doi.org/10.1109/IGARSS.2005.1526688.